NeuroImage: Clinical 31 (2021) 102710

Contents lists available at ScienceDirect

NeuroImage: Clinical

journal homepage: www.elsevier.com/locate/ynicl

White matter integrity of contralesional and transcallosal tracts may predict response to upper limb task-specific training in chronic stroke

Daniela J.S. Mattos [a,*], Jerrel Rutlin [b], Xin Hong [c], Kristina Zinn [f], Joshua S. Shimony [d], Alexandre R. Carter [e]

[a] Department of Neurology, Washington University School of Medicine, Saint Louis, MO 63110, USA
[b] Department of Psychiatry, Washington University School of Medicine, Saint Louis, MO 63110, USA
[c] Department of Genetics, Washington University School of Medicine, Saint Louis, MO 63110, USA
[d] Mallinckrodt Institute of Radiology, Washington University School of Medicine, Saint Louis, MO 63110, USA
[e] Department of Neurology, Washington University School of Medicine, Saint Louis, MO 63110 USA
[f] Department of Radiology, Washington University School of Medicine, Saint Louis, MO 63110, USA

ARTICLE INFO

Keywords:
Diffusion tensor imaging
Stroke rehabilitation
Upper limb
Task specific training
Neuroimaging biomarker
Transcallosal fibers

ABSTRACT

Objective: To investigate white matter (WM) plasticity induced by intensive upper limb (UL) task specific training (TST) in chronic stroke.

Methods: Diffusion tensor imaging data and UL function measured by the Action Research Arm Test (ARAT) were collected in 30 individuals with chronic stroke prior to and after intensive TST. ANOVAs tested the effects of training on the entire sample and on the Responders [ΔARAT $\geq$ 5.8, N = 13] and Non-Responders [ΔARAT $<$ 5.8, N = 17] groups. Baseline fractional anisotropy (FA) values were correlated with ARAT*post* TST controlling for baseline ARAT and age to identify voxels predictive of response to TST. Results.

While ARAT scores increased following training ($p < 0.0001$), FA changes within major WM tracts were not significant at $p < 0.05$. In the Responder group, larger baseline FA of both contralesional (CL) and transcallosal tracts predicted larger ARAT scores post-TST. Subcortical lesions and more severe damage to transcallosal tracts were more pronounced in the Non-Responder than in the Responder group.

Conclusions: The motor improvements post-TST in the Responder group may reflect the engagement of inter-hemispheric processes not available to the Non-Responder group. Future studies should clarify differences in the role of CL and transcallosal pathways as biomarkers of recovery in response to training for individuals with cortical and subcortical stroke. This knowledge may help to identify sources of heterogeneity in stroke recovery, which is necessary for the development of customized rehabilitation interventions.

1. Introduction

Despite advances in acute management, stroke remains the leading cause of chronic motor disability in adults worldwide (Benjamin et al., 2019). The global age-adjusted mortality rates for ischemic and hemorrhagic stroke decreased between 1990 and 2015 (Krishnamurthi et al., 2013; Benjamin et al., 2019). This scenario resulted in substantial increase in the already large number of stroke survivors experiencing motor disability (Krishnamurthi et al., 2013). Current rehabilitation strategies, though they can improve upper limb (UL) motor outcomes, are still lacking as response to training remain suboptimal and highly heterogeneous (Takeuchi and Izumi, 2013; Van Vliet et al., 2012). Studies investigating the neural correlates of specific therapies are scarce. These studies help to clarify how the therapies work, what aspects of brain organization can/cannot be modified, and who is likely to respond.

Lesion location and integrity of motor tracts are key factors influencing motor recovery and response to training post-stroke (Riley et al., 2011; Dromerick and Reding, 1995). For instance, past studies have provided unprecedented insights showing that stroke resulting in

Abbreviations: ARAT, Action Research Arm Test; CL, contralesional; CST, corticospinal tract; FA, Fractional anisotropy; IL, ipsilesional; MCID, minimal clinically important difference; nRESP, non-responder; RESP, responder; TBSS, tract-based spatial statistics; TST, task specific training; UL, upper limb; WM, white matter.

* Corresponding author.
E-mail addresses: juncked@wustl.edu (D.J.S. Mattos), rutlinj@wustl.edu (J. Rutlin), xhong@wustl.edu (X. Hong), shimonyj@wustl.edu (J.S. Shimony), alexandre.carter@wustl.edu (A.R. Carter).

https://doi.org/10.1016/j.nicl.2021.102710
Received 4 December 2020; Received in revised form 25 May 2021; Accepted 26 May 2021
Available online 31 May 2021
2213-1582/© 2021 Published by Elsevier Inc. This is an open access article under the CC BY-NC-ND license (http://creativecommons.org/licenses/by-nc-nd/4.0/).

extensive CST damage, and larger asymmetries of CST integrity, are associated with more severe motor impairments, and reduced global motor function, motor learning, and hand dexterity (Schaechter et al., 2009; Qiu et al., 2011; Stinear et al., 2007). Likewise, individuals with lesion confined to subcortical structures (e.g. basal ganglia) are known to experience worse recovery and are more resistant to treatment than those with cortical lesions (Miyai et al., 1997; Shelton and Reding, 2001). More recently, a larger body of studies has shown evidence for post-stroke brain reorganization in other motor tracts and subsystems extending beyond the CST (Li et al., 2015; Lindenberg et al., 2012; Wadden et al., 2019; Plow et al., 2016). Indeed, the presence of parallel distributed processing in the motor system gives the advantage of multiple options to reconfigure UL motor function (Baker et al., 2015). However, it remains unclear which white matter (WM) tracts critically support UL motor gains following training. Basic information on structural-behavioral correlations post-stroke is crucial to the development of more targeted rehabilitation approaches.

Our main goal was to investigate WM plasticity induced by UL intensive task specific training (TST) in chronic stroke. Stroke patients in this study received higher doses of training than standard conventional training ranging from 3200 to 9600 repetitions for 8 weeks to test for the presence of a dose–response of TST on UL function. Tract-based spatial statistics (TBSS) (Smith et al., 2006) was computed to study potential remodeling of major WM tracts. We hypothesized that improvement in UL function following TST would be correlated with increased WM tract integrity. In addition, given that in our sample some subjects had large motor gains while others did not improve at all, we hypothesized that larger baseline WM integrity would predict increased UL function in response to TST. In addition to our data-driven analysis we performed an ROI-based analysis of transcallosal fibers to further explore the role of WM integrity and interhemispheric interactions in the response to TST.

2. Materials and methods

2.1. Study population

This report includes data from participants with chronic stroke recruited for a phase II, single-blinded, dose–response trial performed at a single site (NCT 01146379) previously published in (Lang et al., 2016). They were included if they met the following inclusion criteria: (1) Ischemic or hemorrhagic stroke as determined by a stroke neurologist; (2) right-handed by self-report; (3) time post stroke of at least 6 months; (4) cognitive skills to actively participate, quantified by scores of 0 to 1 on items 1b and 1c of the National Institutes of Health Stroke Scale (NIHSS); (5) unilateral UL weakness, quantified by a score of 1 to 3 on item 5 (arm item) on the NIHSS; and (6) mild-to-moderate motor function of the affected UL, quantified by a score of 10 to 48 on the Action Research Arm Test (ARAT) (Yozbatiran et al., 2008; Lyle, 1981). They were excluded if they met the following conditions: (1) unavailability for 2-month follow-up; (2) inability to follow two-step commands; (3) psychiatric diagnoses; (4) current participation in other UL stroke treatments; (5) other neurological diagnoses; (6) participants living further than 1 h away and unwilling to travel for assessment and treatment sessions; and (7) pregnancy.

In total, 85 S patients were enrolled in the clinical trial. Thirty-one of these patients underwent diffusion tensor imaging (DTI) scans before training. Out of the 31 patients assessed prior training, two did not repeated the scans after the training. Structural imaging from one participant scanned both prior and after training failed registration and was excluded from the whole analysis. This left 28 participants with DTI measures before and after the training [mean age: 59.43 ± (SD) 10.0 with range of 37 – 82] used for analysis involving changes in UL motor function and DTI post-TST and 30 participants with DTI measures before training [mean age: 59.87 ± (SD) 10.36 with range of 37 – 82] used for predictive analysis of stroke recovery. This research was approved by the Washington University Human Research Protection Office and all participants gave written informed consent prior to participation.

2.2. Study design

Participants were scanned and assessed behaviorally before and after an intervention of TST. The training involved a variety of UL movements including reaching for, moving/manipulating, and releasing objects during a 1 h session, 4 days/week for 8 weeks. Patients were assigned to one of four dose groups with different total number of repetitions of UL tasks: 3,200 (100 repetitions/session; N = 8), 6,400 (200 repetitions/session, N = 5), 9,600 (300 repetitions/session, N = 7), or individualized maximum repetitions (300 repetitions/session and sessions continuing until a stopping criteria was met, N = 10). A detailed description of the study design and the TST has been provided in a previous publication (Lang et al., 2016).

2.3. Outcome measures

The primary outcome measure assessing the UL function following TST was the ARAT test) (Yozbatiran et al., 2008; Lyle, 1981). The ARAT quantifies limitation of the UL function using 19 items divided into four subscales: grasp, grip, pinch, and gross movement. The maximum score of 57 indicates normal performance. The ARAT test was chosen because it is a reliable and valid method to evaluate UL function following stroke and has been widely used in research (Hsieh et al., 1998). Other information reported are: demographic and clinical characteristics: age, sex, race, whether the dominant of the non-dominant side was affected, stroke location, and presence of hemispatial neglect quantified by the unstructured version of the Mesulam Cancellation test (Rengachary et al., 2009).

2.4. Neuroimaging data collection

Scanning was performed with a Siemens 3 T Tim-Trio whole body MRI scanner with a 12-channel head coil including: structural and DTI scans. Structural scans consisted of magnetization prepared rapid gradient echo (MPRAGE) T1-weighted images (TR = 1950 ms, TE = 2.26 ms, flip angle = 9°, voxel size = 1 × 1 × 1 mm, slice thickness = 1 mm) and T2-weighted images (TR = 2500 ms, TE = 435 ms, flip angle = 120°, voxel-size = 1 × 1 × 1 mm, slice thickness = 1.00 mm). The DTI imaging parameters were: single-shot echo planar imaging (EPI), repetition time = 9,200 ms, echo time = 92 ms, single average (NEX = 1), field of view (FOV) = 256 × 256 mm, voxel size = 2 × 2 × 2 mm, 64 contiguous axial slices, flip angle = 90°, 63 directions with $b = 1000$ s/mm^2. Two sequences with $b = 0$ were also collected.

2.5. Lesion segmentation

Stroke lesions were manually segmented on the high resolution MPRAGE of each subject's space using MRIcron software (Robb and Hanson, 1991). All segmentations were reviewed by a board-certified neurologist (AC). Then, the segmented lesions were transformed to Montreal Neurological Institute (MNI) standard and summed at the voxel-wise level to display the number of individuals with structural damage for each voxel at that location (lesion overlay map).

2.6. DTI

DTI images were processed with FMRIB Software Library (FSL, University of Oxford, FSL v5.0.1, www.fmrib.ox.ac.uk/fsl). Standard FSL diffusion processing pipeline (https://fsl.fmrib.ox.ac.uk/fslcourse/lectures/practicals/fdt1/index.html) was used to compute the voxelwise maps of four diffusion indices: fractional anisotropy (FA), mean diffusivity (MD), axonal diffusivity (AD), and radial diffusivity (RD). Most DTI studies of stroke recovery measure FA to estimate general WM integrity, however, other parameters such as AD and RD have also been

used to investigate axonal damage and myelin injury respectively (Fox et al., 2011; Song et al., 2003). MD is an averaged tridimensional measure of water diffusion related to the amount of water in the extracellular space and detection of edema and necrosis (O'Donnell and Westin, 2011).

2.7. Tract-based spatial statistics (TBSS)

Voxel-based statistical analysis of DTI images was performed using TBSS, part of FSL (Smith et al., 2006). First, brain images of participants that received training in their left arm were flipped right-to-left, thereby placing all lesions in the image on the left. Then, the FA volume from each participant was aligned to the within-group target volume that was closest to the group mean using a nonlinear registration algorithm, followed by a 12-degrees of freedom (DOF) affine registration from the target FA volume to the MNI152 template. Residual misalignments between subjects that may happen after the initial nonlinear registrations were minimized by computing a WM skeleton. This process involves morphological thinning of the inter-subject mean FA, and projection of individual's FA values onto a common FA skeleton of major white matter tracts (Smith et al., 2006). The mean FA skeleton representing the centers of all tracts common to the group was generated by setting a map of threshold for voxels with FA values ≥ 0.2. Aligned FA data for each participant were projected onto the standard skeletonized FA image by searching the area perpendicular to each tract for the highest local FA value and assigning this value to the skeleton. A mean FA skeleton was compiled by averaging aligned FA maps for each participant. Finally, the non-linear warps and skeleton projection obtained were applied to MD, AD, and RD.

2.8. ROI-based DTI analysis

We performed a ROI-based DTI analysis to further quantify diffusion characteristics in transcallosal regions. The transcallosal mask was manually drawn using the thickened FA skeleton computed in the TBSS analysis. The mask was divided into 5 parcels using Hofer segmentation (Hofer and Frahm, 2006) with a customized Matlab code. Then, the mean FA was extracted for each parcel of the Hofer segmentation. According to this segmentation regions I-V contain fibers projecting respectively into prefrontal region (region I), to premotor and supplementary motor cortical areas (region II), primary motor cortex (region III), primary sensory cortex (region IV), and finally transcallosal parietal, temporal, and occipital fibers (region V) (Hofer and Frahm, 2006).

2.9. WM tract template

To estimate the percentage of streamlines of specific WM tracts that were lesioned by the stroke, we used a tractography atlas constructed with data from 842 Human Connectome Project (HCP-842 template in MNI152 space) participants available at www.dsi-studio.labsolver.org. The atlas used deterministic fiber tracking (Yeh et al., 2013) to extract 550,000 streamline trajectories that were then reviewed and labeled by experts. The streamline trajectories were segmented into 65 neuroanatomically defined WM tracts. Because we expected that different transcallosal segments might show different relationships to UL function, the transcallosal tract was split into 5 segments based on the Freesurfer's WM segmentation algorithm (Dale et al., 1999) included in DSI_studio. Also, because the reticulospinal tract has been associated with stroke recovery (Owen et al., 2017), the right and left cortico-reticulo-spinal tract were added from the DSI_studio support group. Therefore, there were a total of 72 WM tracts grouped into five categories: projection, transcallosal, association, brainstem, and cerebellar pathways (cranial nerves were not included).

2.10. Statistical analysis

The statistical analysis was divided in three main parts: response to TST (dose–response and overall response to TST), prediction of response to TST, and analyses to compare the RESP and nRESP groups. All statistical analyses were performed in RStudio Version 1.2.1335 and significance was assumed at $p < 0.05$. Normality assumptions were tested and Greenhouse-Geisser correction was applied as needed.

For the dose–response analysis, we performed an ANCOVA with factor dose-group (3,200, 6,400, 9,600, and individualized maximum repetition) for ΔARAT controlling for the effects of baseline ARAT. Then, given the absence of dose–effect on ΔARAT, mean differences between baseline ARAT and ARAT post-TST were compared using paired *t*-test. Finally, to investigate brain changes associated with TST, we performed a *Pearson* correlation between ΔFA and ΔARAT controlling for age and prediction of response to TST.

For the predicted response to TST, the main analysis was performed at the voxel-wise level. A *Pearson* correlation was conducted as a follow up analysis to determine the strength of this correction. Then a ROI-based analysis was conducted to determine whether transcallosal fibers were predictive of response to TST. At the voxel-wise level (within the region defined by the TBSS FA skeleton), the relationship between baseline DTI and ARAT*post* (indicating response to TST) was examined using *Pearson* correlation with baseline ARAT and age as covariates using the FSL *Glm* statistical model, similarly to previous research (Cassidy et al., 2018). Multiple comparison corrections were applied using a permutation based statistical approach (N = 5000) within FSL "randomize" program using the threshold-free cluster enhancement method (Smith et al., 2006). For the follow up analysis, the average FA at baseline of all predictive voxels from the prior analysis was calculated for each subject. The strength of the relationship between these baseline FA values and ΔARAT was expressed by calculating a *Pearson* correlation coefficient. Lastly, we defined transcallosal ROIs using the Hoffer parcellation and computed *Spearman* correlations between baseline FA and 1) baseline ARAT, 2) ARAT post-TST, and 3) ΔARAT.

To investigate differences between the RESP and nRESP groups at baseline, we performed two analyses. In the first one, we compared the demographic and clinical characteristics of the RESP and nRESP groups using either Chi-square or t-tests, and their lesion distribution. In the second one, we calculated the percentage of streamlines that intersected with lesioned voxels by each subject's stroke. The streamlines and category of tracts was determined based on the HCP842 tractography (Yeh et al., 2018) atlas. The mean percentage of streamlines with lesioned voxels was computed for each tract category and divided into four bins : 0–25%, 26–50%, 51–75%, and 76–100% to indicate the severity of tract damage in the RESP and nRESP groups at baseline and post-training.

3. Results

3.1. Participant characteristics

Participants' characteristics are shown in Table 1. Fig. 1 shows a voxel-wise average of the segmented lesions normalized to a standard MNI-152 brain template. Seventy percent of strokes were subcortical (N = 18/26) localized in the ipsilesional (IL) basal ganglia, thalamus, and WM fibers. In 28% of the cases, lesions were both subcortical and cortical (N = 8/26) and occurred predominantly within the middle cerebral artery distribution. In four individuals no lesion could be identified. The average lesion volume was 15,262 mm^3 (1,908 voxels of 2 × 2 × 2 mm).

3.2. Response to TST

3.2.1. Dose-Response to TST

The ANCOVA showed no significant dose–response for ΔARAT ($F_{3,1}$

Table 1
Participant's characteristics.

	ID	Age	Sex	Race	Education	Arm Trained	Mesulam	Baseline ARAT	ARATpost	ΔARAT	Lesion Volume (mm^3)	Lesion Location
1	03	60	F	Afr. Amer.	NA	Dom	1	39	57	18	2452	L CR & BG / R BG
2	22	54	M	Afr. Amer.	HS	Dom	1	41	57	16	29,178	Bil Cerebellar Hemisphere (R > L)
3	34	53	F	Caucasian	< College	Dom	0	40	55	15	NA	Not identifiable
4	01	37	M	Afr. Amer.	HS	Dom	15	27	40	13	48,240	L Frontal/Parietal/Insula/ Occipital (C + S); L thalamic & BG lacune / Bilateral cerebellar lacune
5	24	82	M	Caucasian	NA	Dom	0	16	27	11	90,095	L Frontal/Parietal/Temporal/ Insula (C + S); L CR and BG
6	44	48	F	Afr. Amer.	< College	Dom	2	40	49	9	482	L CR, Thalamus, BG, genu of the internal capsule;R PLIC lacune
7	02	60	F	Caucasian	< College	Dom	0	31	40	9	35,646	L Frontal/Parietal (C + S); L Insula (C)
8	19	61	M	Afr. Amer.	HS	Dom	0	39	47	8	5124	L Frontal (S), CC, CR, BG, thalamus, ALIC, L middle cerebellar peduncle / R VA thalamus lacune; pons
9	38	59	F	Caucasian	< College	Dom	1	48	55	7	61	L genu of the internal capsule
10	08	60	M	Afr. Amer.	< College	Non-Dom	3	39	46	7	434	R CR & BG / L CR & cerebellum
11	43	56	M	Caucasian	HS	Non-Dom	1	37	44	7	13,118	R parietal/posterior insula (C + S)
12	35	65	M	Afr. Amer.	< College	Dom	26	32	38	6	1562	L prefrontal (S), multiple bilateral thalamic and BG lacunes and L pons
13	12	58	M	Afr. Amer.	HS	Dom	0	30	36	6	463	L Frontal/Parietal (C + S) / R Frontal/Temporal (C + S)
14	41	54	M	Caucasian	HS	Non-Dom	2	38	43	5	72,119	R Frontal/Parietal/Temporal/ Insula (C + S), thalamus, and basal ganglia
15	18	70	M	Afr. Amer.	HS	Dom	5	37	42	5	7108	L frontal (S), CR, PLIC, thalamus, and BG
16	30	56	M	Caucasian	< College	Dom	0	25	30	5	134	L PLIC
17	33	50	M	Caucasian	HS	Dom	0	38	42	4	7209	L CR, BG, subinsula
18	27	42	F	Caucasian	HS	Non-Dom	2	33	37	4	12,757	R CR, BG, insula (C + S), medial temporal lobe
19	40	79	NA	NA	< College	Dom	2	31	35	4	NA	Not identifiable lesion
20	17	77	F	Afr. Amer.	NA	Dom	12	10	14	4	386	L pontine / R BG and thalamic lacune
21	10	52	M	Afr. Amer.	HS	Non-Dom	0	13	15	2	12,631	R frontal (S) CR & BG, superior occipital frontal fasciculus / L cerebellar lacune / L thalamic lacune
22	13	60	F	Afr. Amer.	HS	Non-Dom	0	10	12	2	981	R CR & BG
23	37	66	F	Afr. Amer.	< College	Non-Dom	0	38	39	1	884	R thalamus
24	26	60	M	Caucasian	< College	Non-Dom	1	38	39	1	413	L Thalamus / PLIC
25	20	53	F	Afr. Amer.	NA	Dom	3	37	38	1	NA	Not identifiable lesion
26	23	66	F	Caucasian	VS/TS	Dom	1	36	37	1	910	L thalamus & BG lacune, cerebral peduncle
27	21	54	M	Caucasian	< College	Non-Dom	8	39	39	0	NA	Not identifiable lesion
28	45	79	M	Caucasian	NA	Non-Dom	6	17	17	0	791	L insular cortex (S), CR
29	09	64	F	Afr. Amer.	HS	Dom	5	33	31	−2	38,940	L parietal/temporal/occipital (C + S), cerebellum, thalamus-pulvinar, and PLIC / R internal capsule
30	11	61	M	Caucasian	< College	Non-Dom	0	32	29	−3	233	L pontomedulary junction / inferior cerebellar peduncle
Summary Mean ± SD		59.87 ± 10.36	17 M, 12F, 1NA	15 Afr. American 14 Caucasian 1NA	12 HS 1 VS/TS 12 < College 5NA	21 Dom, 9 Non-Dom	3.23 ± 5.63	32.13 ± 9.80	37.67 ± 11.86	5.53 ± 5.20	14705.81 ± 23449.36	18 (S), 8 (C + S), 4NA

Legend: Afr. Amer. = African American, Dom = Dominant, Non-Dom: Non-Dominant, IM = Individualized Maximum, HS = High School, VS/TS = Vocational School / Technical School. R = Right, L = Left, MCA = Middle Cerebral Artery, PCA = Posterior Cerebral Artery, PLIC = Posterior Limb of the Internal Capsule.
C = cortical, S = subcortical, CR = corona radiata, BG = basal ganglia, ALIC = anterior limb of the internal capsule, PLIC = posterior limb of the internal capsule, VA = ventral anterior nucleus.

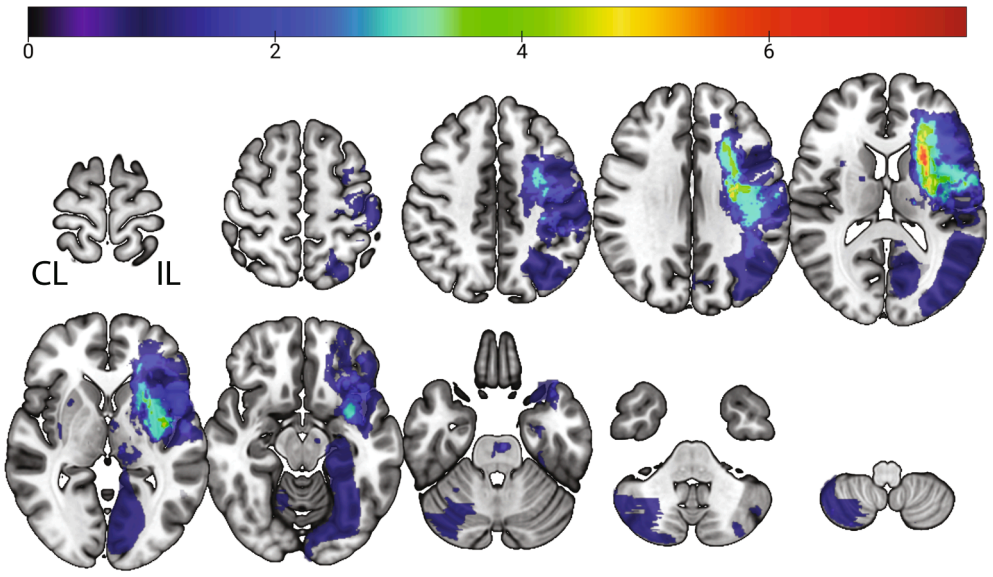

Fig. 1. Overlap of lesion location for all participants. Images of participants that received training in their left arm were flipped around the midsagittal plane. In 4 participants (20, 21, 34, and 40 subject's IDs in Table 1), no lesion was identified in the images, N = 26. Images are in Neurological convention. IL = ipsilesional, CL = contralesional.

= 0.880, $p = 0.466$, Supplementary Fig. 1). The mean ± SD change in ARAT score for each intervention group was: 3,200: 4.43 ± 3.15; 6,400: 4.40 ± 2.88; 9,600: 5.86 ± 6.41, and Individualized Maximum: 7.89 ± 6.41. These values were slightly below those reported for the larger cohort that ranged between 5.1 and 8.4 points (Lang et al., 2016). When the dose groups were combined, the mean ARAT score increased significantly following TST (PRE: 32.23 ± 9.80 and POST: 37.67 ± 12.06, $t_{29} = 5.8235$; $p < 0.0001$, 95%CI: 3.59–7.48, Fig. 2A). This mean

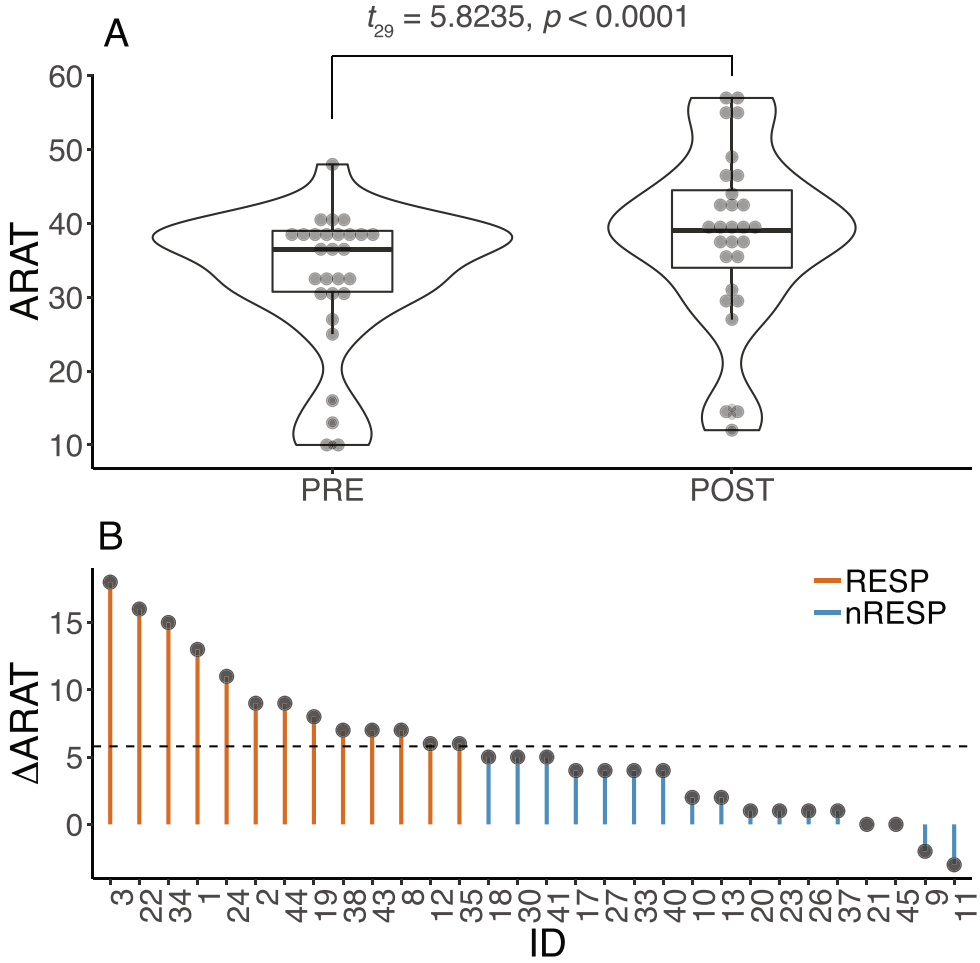

Fig. 2. A) Box plots with an outline of the probability density showing values of ARAT score pre- and post- task specific therapy for all participants (N = 30). B) Values of changes in ARAT scores following task-specific therapy for each participant illustrating the variability of response from therapy. The dotted line indicates the minimal clinically important difference (MCID) of 5.8 for ARAT score that was used to classify the participants into Responders (greater than5.8, N = 13) and Non-Responders (<5.8, N = 17).

increase of 5.53 ± (SD) 5.20 points is close to the MCID value of 5.8.

3.2.2. Overall response to TST

The focus of this research was to investigate brain changes either associated with or predictive of response to TST. Thus, given the absence of a significant dose–effect on ARAT score, we did not investigate effects of dose of TST on DTI-related measures. The overall effect of the TST on UL function was not accompanied by changes in FA, MD, AD, and RD at $p = 0.05$ as quantified by TBSS. In summary, there was an increase in ARAT, but no change in DTI measures.

3.3. Prediction of response to TST

3.3.1. Baseline FA in TBSS predicts UL response to TST in the RESP groups

The response to TST was highly heterogeneous. As can be observed in Fig. 2B, while ΔARAT was<5.8 for 17 participants (nRESP group), it was larger than 5.8 for 13 participants (RESP group). Our next question was whether the integrity in specific WM tracts was predictive of UL response to TST. Because our main research goal was to understand and predict response to training, we performed further analysis with the RESP group.

At the whole brain voxel-wise level, voxels significantly associated with response to TST for the RESP group is shown in both Fig. 3A for FA and Supplementary Fig. 2A for MD, AD, and RD. In summary, larger baseline FA, and smaller baseline MD, AD, and RD significantly predicted improvement in UL function quantified by ARAT*post* controlling for baseline ARAT and age. Predictive voxels were located in the CL (untrained) hemisphere and in transcallosal tracts. Fig. 3B shows that the linear regression between baseline FA and ΔARAT was significant ($R = 0.75$, p-value = 0.0033) for the RESP group and not significant for the nRESP group ($R = -0.16$, p-value = 0.54). In the RESP group, the pathways with the largest percentage of streamlines containing voxels whose baseline FA was predictive of response to TST included CL association pathways (inferior fronto-occipital cortex, middle and superior longitudinal fasciculus, arcuate fasciculus, extreme capsule, and uncinate fibers), projection pathways (optic radiation, corticostriatal, and fronto, parieto, temporo, and occipito-pontine fibers), and transcallosal pathways (Supplementary Fig. 2B).

3.3.2. Baseline FA in some transcallosal ROIs correlated with UL post TST in RESP

The principle pathway by which the CL hemisphere can exert its influence on the hemiparetic UL is by transcallosal fibers. We performed a correlational analysis between baseline FA and 1) baseline ARAT, 2) ARAT*post*, and 3) ΔARAT in 5 transcallosal ROIs. Results from CC_I, CC_{II}, and CC_{IV} are illustrated in Fig. 4, and results from CC_{III} and CC_V are not shown. At baseline, ARAT score did not correlate with FA in any CC region (Fig. 4, upper row). However, for the RESP group, a correlation developed after training in that a larger ARAT*post* following TST was correlated with larger baseline FA values within CC_I, CC_{II}, and CC_{IV} (Fig. 4, lower row). Baseline FA values within CC_{III} were not significantly correlated with baseline ARAT (RESP: $\rho = 0.3$, $p = 0.4$; nRESP: $\rho = -0.02$, $p = 0.9$) or with ARAT*post* (RESP: $\rho = 0.3$, $p = 0.3$; nRESP: $\rho = -0.2$, $p = 0.5$). Similarly, baseline FA values within CC_V were not significantly correlated with baseline ARAT (RESP: $\rho = 0.3$, $p = 0.3$; nRESP: $\rho = -0.2$, $p = 0.4$) or with ARAT*post* (RESP: CC_V: $\rho = 0.5$, $p = 0.1$; nRESP: $\rho = -0.3$, $p = 0.2$). Also, baseline FA was not significantly predictive of ΔARAT at $p < 0.05$. These findings suggest a role for interhemispheric interactions in UL function post training. However, they do not support transcallosal FA in isolation as a prognostic biomarker of response to TST or in distinguishing the RESP from the nRESP group at baseline.

3.4. Lesion location and lesioned WM tracts may distinguish the RESP from the nRESP group.

The RESP and nRESP groups were well matched in terms of age, sex, race, level of education, whether the stroke affected the dominant or the non-dominant arm, the level of UL function quantified by the ARAT score, and lesion volume (Table 2). Fig. 5 shows the contrast and overlap images of binarized lesion location with a threshold ≥ 1 for the RESP and nRESP groups. While the RESP group had predominantly rostral/cortical lesions, the nRESP group had predominantly caudal WM and subcortical lesions affecting thalamus, basal ganglia, and internal capsule. In Table 3 we present the mean % of streamlines with lesioned voxels for the RESP and nRESP groups across WM tract category and for IL CST. Transcallosal pathways were more extensively lesioned in the nRESP than in the RESP group (Table 3 and Supplementary Fig. 3). The % streamlines of IL CST was not different in both the RESP and nRESP groups which may be expected given the comparable ARAT scores between groups at baseline.

4. Discussion

Individuals with chronic stroke experienced gains in UL function after intensive TST. However, these motor gains were not accompanied by microstructural changes within major WM pathways. We observed a heterogeneous response to TST, which led to the post-hoc hypothesis that baseline WM microstructure predicts motor response following TST. TBSS analysis showed that larger UL gains were predicted by larger baseline WM integrity of fibers located predominantly within the CL hemisphere, but only in the subgroup of RESP. While it may seem that

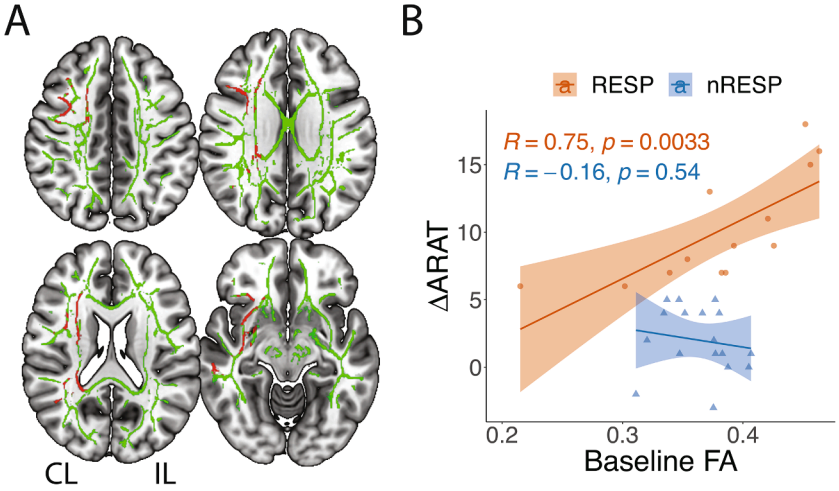

Fig. 3. A) Voxels in green represent the white matter skeleton for Responders on a MNI-152 template. Voxels in red represent significant correlation (corrected $p < 0.05$) between baseline FA and ARAT*post* scores controlling for baseline ARAT and age for Responders (N = 13). B) Pearson, R, correlation between averaged baseline FA values and changes in ARAT score (ΔARAT) for both Responders (RESP, N = 13) and for non-Responders (N = 17). For both groups, averaged baseline FA values was extracted from all significant voxels in the TBSS analysis (shown in red in Fig. 3A). (For interpretation of the references to colour in this figure legend, the reader is referred to the web version of this article.)

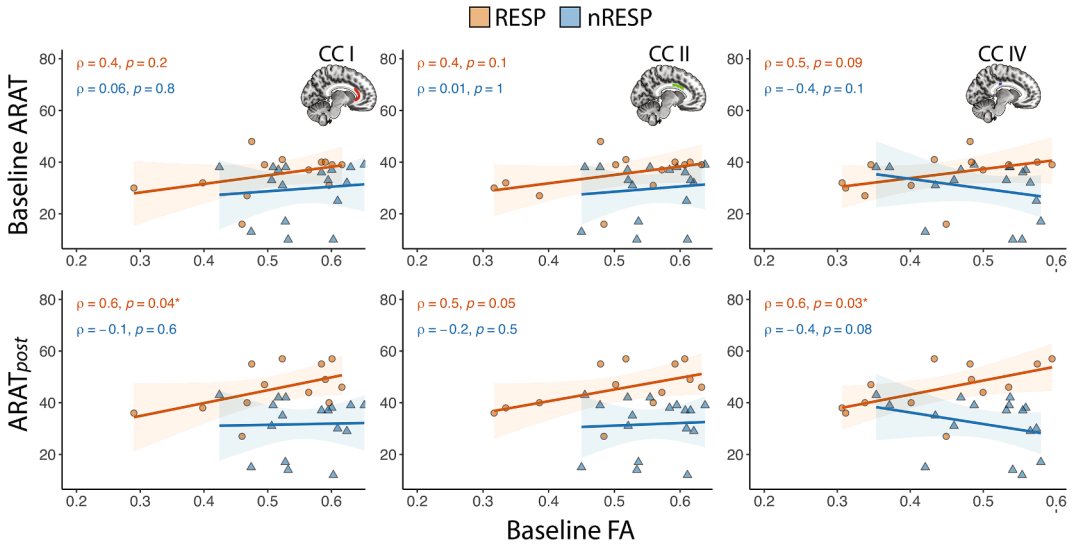

Fig. 4. Spearman (ρ) correlation between baseline FA values extracted from transcallosal ROIs and both baseline ARAT score and ARAT*post* for Responders (RESP, N = 13) and Non-Responders (nRESP, N = 17). ROIs were defined using Hofer segmentation, regions I, II and IV contain fibers projecting respectively into prefrontal region (region I), to premotor and supplementary motor cortical areas (region II), and to primary sensory cortex (region IV) (Hofer and Frahm 2006).

Table 2
Comparison between the Responder (RESP) and non-Responder (nRESP) groups.

	RESP (n = 13)	nRESP (n = 17)	p-value*
Age (yrs)	57.92 ± 10.14	61.35 ± 10.59	0.376
Sex	8 M, 5F	9 M, 7F, 1NA	1.000
Race	8 Afr. American	7 Afr. American	0.462
	5 Caucasian	9 Caucasian	
		1NA	
Dom vs. Non-Dom	11 Dom, 2 NDom	10 Dom, 7 NDom	0.229
Education	5 HS	7 HS	1.000
	0 VS/TS	1 VS/TS	
	6 < College	6 < College	
	2NA	3NA	
Mesulam	3.86 ± 7.78	2.76 ± 3.42	0.646
Baseline ARAT	35.31 ± 8.07	29.71 ± 10.53	0.110
ΔARAT	10.15 ± 4.08	2.20 ± 2.54	**<0.001**
Lesion Volume	18904.58 ± 27773.48	11106.86 ± 20416.37	0.209

*From comparisons between groups using Chi square tests for categorical data and *t*-tests for continuous data.
Legend: M = Male, F = Female, Afr. American = African American, Dom = Dominant, Non-Dom: Non-Dominant, IM = Individualized Maximum, HS = High School, VS/TS = Vocational School / Technical School. R = Right, L = Left, RESP: Responder, nRESP: Non-Responders. N = 30.

this relationship is an artifact necessarily resulting from focusing only on RESP, the null hypothesis was that baseline FA values would be randomly distributed with respect to response to therapy. Our results disprove this null hypothesis. Importantly, while TBSS and ROI analyses did not distinguish the RESP and nRESP groups at baseline, a qualitative analysis of the lesion distribution suggested that the category of damaged tracts may be predictive of response to training. More specifically, our data suggests that the nRESP group had more subcortical lesions and more severe damage to transcallosal tracts than the RESP group, which may have interfered with additional gains post-TST. Below we discuss the major implications of the findings from this study.

4.1. Increase in UL function post-TST

UL function measured with the ARAT increased significantly following 8 weeks of TST. The number of repetitions in this study represents a very large increase in dose compared to the number of repetitions documented during standard rehabilitation (Carey et al., 2002; Boyd and Winstein, 2006). However, the ARAT increase was still only on the order of the MCID, suggesting that if a dose response curve does exist, even 10,000 repetitions may lie within the flattened lower range of a likely sigmoid-shaped dose–response curve. This amount of response to TST is similar to previous reports on UL interventions provided at the chronic stage (Bundy et al., 2017), but smaller than more recent studies that tested very high doses of training (Daly et al., 2019; McCabe et al., 2015). Alternatively, lack of dose–response could reflect a ceiling effect, however more recent studies that tested very high doses of training in chronic stroke (Daly et al., 2019; McCabe et al., 2015) suggest that larger behavioral improvements are possible with larger doses of therapy.

4.2. Mechanisms of improved UL function in response to TST

We investigated whether UL motor response to TST was associated with underlying plasticity of the WM microstructure. Structural changes in WM have been previously shown after training (Draganski and May, 2008). Training-induced plasticity associated with arm function in individuals with stroke may involve the use of alternate motor, transcallosal, or even non-motor fibers (Choudhury et al., 2019; Baker et al., 2015). In *subacute stroke*, larger FA in CST, alternate motor fibers (such as cortico-rubro-spinal and cortico-reticulo-spinal tract) and transcallosal fibers were positively correlated with larger treatment response (Song et al., 2015; Young et al., 2016). By contrast, in *chronic stroke*, the current literature lacks evidence for structural plasticity following motor training (Borich et al., 2014; Rickards et al., 2014; Sterr et al., 2014). For instance, two studies showed gains in the use of the UL following constraint-induced movement therapy that were not associated with changes in CST integrity (Rickards et al., 2014; Sterr et al., 2014). Similarly, we failed to show an association between UL response to TST and microstructural WM changes. However, improvements following intensive speech therapy in chronic stroke have been associated with training-induced WM plasticity (Schlaug et al., 2009; Allendorfer et al., 2012; Wan et al., 2014). In Wan et al. (2014), FA decrease in right-hemisphere regions was associated with improvement in speech production. Earlier report showed correlations of speech production with larger fiber number and volume in the left arcuate fasciculus (Schlaug et al., 2009). Thus, conclusions from the positive results following training of other systems even at the chronic stage should not be extrapolated to the motor system. Although brain structure measured with DTI is claimed to be a stronger predictor of chronic recovery than inter-hemispheric functional connectivity (Lin et al., 2018; Qiu et al., 2011), the absence of WM change post-training suggests that the major

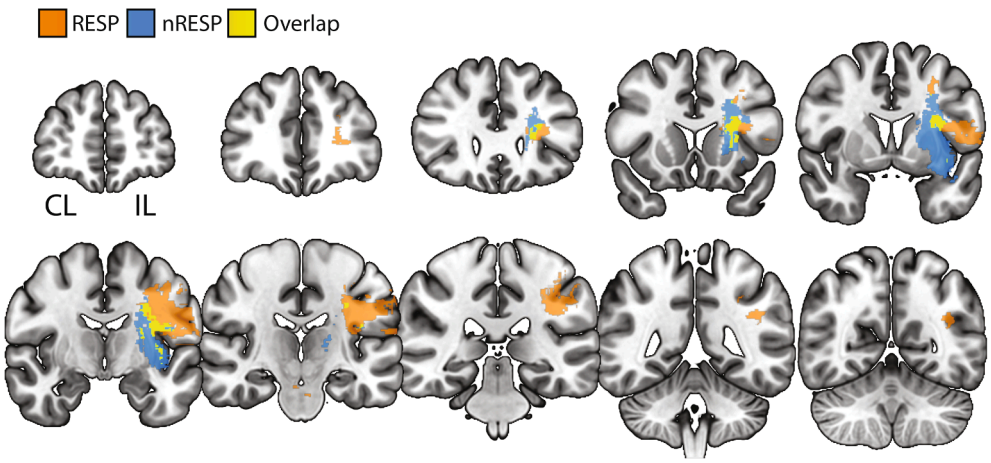

Fig. 5. Contrast and overlap images of binarized lesion location for Responders (RESP) and non-Responders (nRESP) thresholded at ≥ 1. RESP had a more rostral/cortical lesions and nRESP had a more caudal white matter and subcortical lesions affecting thalamus, basal ganglia, and internal capsule. Images are in Neurological convention, N = 26.

Table 3
Descriptive table with mean percentage of streamlines interrupted by lesioned voxels. Tracts count are in parenthesis. RESP: Responder (N = 12) and nRESP: non-Responder (N = 14). Total number of subjects is 26 because 4 subjects had non-identifiable lesion in Table 1.

Lesioned Streamlines	Group	Projection	Transcallosal	Association	Brainstem	Cerebellum	CST, IL
0%	RESP	0.00 (229)	0.00 (70)	0.00 (245)	0.00 (147)	0.00 (69)	0.00 (7)
	nRESP	0.00 (257)	0.00 (76)	0.00 (286)	0.00 (166)	0.00 (93)	0.00 (5)
1–25%	RESP	9.24 (32)	10.75 (16)	5.76 (21)	9.95 (21)	6.28 (18)	0.00
	nRESP	9.21 (38)	7.47 (17)	10.00 (18)	9.20 (28)	3.09 (11)	9.67 (3)
26–50%	RESP	49.52 (15)	32.20 (5)	37.34 (6)	28.54 (11)	46.00 (1)	31.50 (2)
	nRESP	44.71 (21)	38.86 (7)	37.28 (7)	29.92 (11)	33.00 (1)	41.75 (4)
51–75%	RESP	58.80 (5)	0.00	64.00 (6)	60.00 (1)	65.50 (2)	57.67 (3)
	nRESP	66.17 (6)	69.67 (3)	62.00 (6)	68.00 (2)	0.00	63.50 (2)
76–100%	RESP	87.80 (5)	0.00	87.75 (8)	78.00 (1)	80.00 (1)	76.00 (1)
	nRESP	89.11 (9)	94.00 (2)	91.60 (3)	0.00	0.00	80.00 (2)

mechanism targeted by TST and underlying observed motor gains is non-structural as detected with MRI. This should be investigated further.

4.3. Prediction of response to TST

The finding that most voxels predictive of the size of response to TST lie CL to the damaged hemisphere for the RESP group was not expected. However, this observation is not without precedent as the CL hemisphere has long been hypothesized to be involved in stroke recovery (Simis et al., 2015; Dodd et al., 2017; Buetefisch, 2015; Chen et al., 2019). For instance, CL PLIC FA was significantly correlated with multiple dimensions of motor recovery (e.g. level of physical impairment, grip strength, and hand dexterity) in chronic stroke (Borich et al., 2012). Progressive activation of the CL hemisphere has been recently associated with the expression of atypical flexor synergies (McPherson et al., 2018) and the use of use alternate motor pathways to support UL function (Owen et al., 2017). There has been a heated debate in the field on whether the CL hemisphere is associated with positive or negative response to training, and for which subgroups of stroke patients (Li et al., 2019; Dodd et al., 2017; Buetefisch, 2015). Our results agree with the notion that the CL hemisphere supports UL recovery for a subset of chronic stroke patients.

In addition to the TBSS evidence implicating CL hemispheric and transcallosal pathways, our ROI-based analysis supports an involvement of transcallosal fibers in the RESP group. Reduced integrity of transcallosal fibers has been frequently associated with poor arm recovery (Wang et al., et al., 2012; Stewart et al., 2017; Hayward et al., 2017; Jang et al., 2009; Li et al., 2015). However, many fewer studies have examined the value of transcallosal pathways in predicting the motor response to training (Lindenberg et al., 2012). Lindenberg et al. (2012) showed that integrity of transcallosal fibers are better predictors of UL gains following training than IL CST (Lindenberg et al., 2012). Although our ROI analysis failed to show that transcallosal ROIs were predictive of the response to therapy, we observed the development of a significant correlation between FA and ARAT in 3 of 5 segments of the corpus callosum post treatment which was not present prior to training. This observation supports the interpretation that interhemispheric communication is important for UL motor function in TST. ROIs CC-I, CC-II, and CC-IV contain fibers from prefrontal, premotor and supplementary motor areas, and primary sensory pathways respectively suggesting a possible role for executive function, motor planning, and sensory based-feedback in the response to TST.

The result of a predictive role for non-motor CL hemispheric tracts (Fig. 2 and Supplementary Fig. 2) raises the possibility that other WM pathways are facilitating TST-related improvement. More specifically, in addition to the transcallosal fibers, several association fibers classically related to language function were predictive of UL motor gain such as superior longitudinal fasciculus and arcuate fasciculus, the uncinate fasciculus, extreme capsule, middle longitudinal fasciculus, inferior longitudinal fasciculus and inferior fronto-occipital fasciculus (Dick and Tremblay, 2012). While this finding was unexpected, activity of higher-order visuo-motor control is suggested to be independent of that of the primary motor cortex (Gregory Króliczak et al., 2016). Moreover, homotopic recruitment is a well-known mechanism of recovery post-stroke. It is possible that homotopic language pathways also support praxis, given the strong correlation between these two fundamental cognitive abilities that may share common cerebral specialization (Grzegorz Króliczak et al., 2020). Importantly, we also reported streamlines with predictive voxels in WM tracts connecting pons and striatum to frontal, parietal, temporal, and occipital cortex. The full

repertoire of UL behavior depends on cortico-subcortical circuits that consist not only of projection fibers from primary motor cortex, but also tracts supporting higher-order cognition associated with feedforward and feedback-based control (Xu et al., 2015). Integration of higher-order pathways and subcortical regions from the intact hemisphere may facilitate motor learning strategies targeted by TST rehabilitation. The predictive power of baseline DTI for magnitude of motor gain post-TST in the RESP group may seem incongruent with its inability to distinguish the RESP from the nRESP group. This discrepancy might be explained by the level of engagement of CL pathways in these two groups. It may be only under conditions involving CL recruitment that CL WM integrity comes into play.

4.4. Lesion anatomy and response to TST

Both the RESP and the nRESP groups were well matched in terms of demographic characteristics including their baseline ARAT score, age, and sociodemographics. Therefore, information acquired from brain imaging might be invoked to explain their failure to respond to TST. A qualitative evaluation of stroke anatomic lesion distribution in our sample shows a striking difference between the RESP group with more rostral/cortical lesions, and the nRESP group with more caudal WM and subcortical lesions affecting the thalamus, basal ganglia and internal capsule. In Table 3 and Supplementary Fig. 3 we showed that transcallosal fibers were more extensively lesioned in the nRESP group than in the RESP group.

A growing body of evidence suggests that patients with subcortical lesions have deficits that are more severe and longer lasting than do individuals with cortical lesions (Miyai et al., 1997; Shelton and Reding, 2001). For example, a neuroimaging study by Shelton and Reding (2001) demonstrated that recovery of isolated UL movements was more likely for individuals with purely cortical stroke (involving supplementary motor area, premotor cortex or primary motor cortex) compared with a subcortical or mixed cortical/subcortical group. Likewise, subcortical stroke participants of the ICARE clinical trial who received a higher dose of UL training achieved 2–3 points less recovery from impairment than controls (Edwardson et al., 2019). In contrast, those with cortical or mixed lesions experienced ~ 7 points more recovery than controls (Edwardson et al., 2019). Thickbroom et al. (2015) showed that larger UL impairment was associated with increased M1 CL excitability for patients with subcortical stroke, which was not observed for cortical stroke. In their study that did not include imaging, it was the relationship between behavior and electrophysiology rather than their baseline values that differentiated both groups. All together, these findings suggest that patients with subcortical WM lesions may be less responsive to task-based therapies alone. Patients with this type of lesion may require adjunct interventions such as non-invasive brain stimulation or pharmacological agents or may respond to completely different interventions such as training with a brain-computer interface driven by signals from the CL hemisphere (Bundy et al., 2017). It is also likely that some individuals with damage to critical pathways will not experience gains in UL function with any therapy. Whether resistance to training is due to damage to their WM as opposed to the effects of damage to thalamus and basal ganglia deserves further investigation.

4.5. Study limitations

Due to the nature of stroke, it is possible that some of the variability observed in baseline WM integrity may reflect diffuse changes due to vascular compromise (Hamanaka et al., 2018a; 2018b). In four individuals no lesion could be identified. In the chronic stage of stroke, it can be difficult to distinguish what were initially small lacunar strokes from the non-specific changes typical of small vessel disease that are of unclear behavioral significance. In addition, the hematoma of a hemorrhagic stroke, while obvious at the acute stage, is resorbed in time sometimes leaving behind only a fraction of the volume of the initial lesion which can blend in with the other changes seen in small vessel disease. Residual hemosiderin is not identifiable in T1-weighted or standard T2 MRI scans, and a T2*-weighted sequence used to depict hemosiderin was not acquired in this study. It is unlikely that the presence of these "lesion-negative" subjects would have influenced the interpretation of our results as lesioned voxels were not excluded from WM analysis and as the predictive value of baseline FA was restricted to the non-lesioned hemisphere and transcallosal tracts. It is possible that our failure to observe training-dependent structural changes in WM integrity relates to factors affecting the signal to noise ratio such as small sample size, stroke heterogeneity within our sample, and type of analysis. Our sample size was small with heterogeneous characteristics (cortical and subcortical lesions, variable lesion sizes, participants with previous history of stroke) and likely contributed significantly to inter-individual variability in response to TST. The small sample size also limited exploring statistical tests with robust models including multiple ROIs of interest and their interactions. Also, we did not use an impairment level measure such as the UL Fugl-Meyer or arm kinematics and indices of motor coordination which may have been better correlated with our structural measures of WM integrity. Outcome measures of UL motor function with a higher level of granularity may be used to distinguish motor from non-motor pathways supporting UL function. This may be necessary to further investigate pathways specifically associated with atypical synergies or dexterity. Finally, delivering an even larger dose of training (Supplementary Fig. 1), possibly by using a protocol similar to Daly et al. (2019), might have facilitated the detection of neural correlates of improvement by achieving an even greater effect size on behavior and increasing the number of subjects in the RESP group.

5. Conclusion

In this study of the neural correlates of motor improvement after TST of the UL in chronic stroke, we found no evidence of WM plasticity. We suggest that neural correlates of larger doses of treatment should be investigated. There was significant heterogeneity in the response to TST allowing for the characterization of the RESP and nRESP groups. In the RESP group, larger motor gains following TST were associated with larger baseline WM integrity within CL hemisphere motor and non-motor pathways and transcallosal fibers. In addition, transcallosal tracts were more frequently lesioned in the nRESP group. These findings suggest that the response to TST in the RESP group may reflect the engagement of interhemispheric processes to which the nRESP group does not have access. Future studies should include CL and transcallosal FA as biomarkers to better characterize spontaneous recovery and response to training in cortical and subcortical stroke. This knowledge may help to identify sources of heterogeneity post-stroke, which is a necessary condition for the development of customized rehabilitation interventions.

CRediT authorship contribution statement

Daniela J.S. Mattos: Conceptualization, Formal analysis, Writing - original draft, Visualization. **Jerrel Rutlin:** Software, Data curation. **Xin Hong:** Investigation. **Joshua S. Shimony:** Investigation. **Alexandre R. Carter:** Conceptualization, Methodology, Resources, Writing - review & editing, Supervision, Funding acquisition.

Declaration of Competing Interest

The authors declare that they have no known competing financial interests or personal relationships that could have appeared to influence the work reported in this paper.

Acknowledgments

The work was supported by R01 HD068290 and the Department of Neurology at Washington University School of Medicine. The authors thank Dr. Catherine Lang, PT, PhD, Professor of Physical Therapy, Neurology, and Occupational Therapy at Washington University School of Medicine and her team for conducting the training and collecting all the behavioral data. JSS was supported by the Eunice Kennedy Shriver National Institute Of Child Health & Human Development of the National Institutes of Health under Award Number U54 HD087011 to the Intellectual and Developmental Disabilities Research Center at Washington University.

Appendix A. Supplementary data

Supplementary data to this article can be found online at https://doi.org/10.1016/j.nicl.2021.102710.

References

Allendorfer, J.B., Storrs, J.D.M., Szaflarski, J.P., 2012. Changes in White Matter Integrity Follow Excitatory RTMS Treatment of Post-Stroke Aphasia. Restor. Neurol. Neurosci. 30 (2), 103–113. https://doi.org/10.3233/RNN-2011-0627.

Baker, S.N., Zaaimi, B., Fisher, K.M., Edgley, S.A., Soteropoulos, D.S., 2015. Pathways mediating functional recovery. Prog. Brain Res. 218 (April), 389–412. https://doi.org/10.1016/bs.pbr.2014.12.010.

Benjamin, E.J., Muntner, P., Alonso, A., Bittencourt, M.S., Callaway, C.W., Carson, A.P., Chamberlain, A.M., Chang, A.R., Cheng, S., Das, S.R., Delling, F.N., Djousse, L., Elkind, M.S.V., Ferguson, J.F., Fornage, M., Jordan, L.C., Khan, S.S., Kissela, B.M., Knutson, K.L., Kwan, T.W., Lackland, D.T., Lewis, T.T., Lichtman, J.H., Longenecker, C.T., Loop, M.S., Lutsey, P.L., Martin, S.S., Matsushita, K., Moran, A.E., Mussolino, M.E., O'Flaherty, M., Pandey, A., Perak, A.M., Rosamond, W.D., Roth, G. A., Sampson, U.K.A., Satou, G.M., Schroeder, E.B., Shah, S.H., Spartano, N.L., Stokes, A., Tirschwell, D.L., Tsao, C.W., Turakhia, M.P., VanWagner, L.B., Wilkins, J. T., Wong, S.S., Virani, S.S., 2019. Heart Disease and Stroke Statistics-2019 Update: A Report From the American Heart Association. Circulation 139 (10). https://doi.org/10.1161/CIR.0000000000000659.

Borich, Michael R., Brown, Katlyn E., Boyd, Lara A., 2014. Motor Skill Learning Is Associated with Diffusion Characteristics of White Matter in Individuals with Chronic Stroke. Journal of Neurologic Physical Therapy. https://doi.org/10.1097/NPT.0b013e3182a3d353.

Borich, M.R., Mang, C., Boyd, L.A., 2012. Both Projection and Commissural Pathways Are Disrupted in Individuals with Chronic Stroke: Investigating Microstructural White Matter Correlates of Motor Recovery. BMC Neuroscience 13 (1), 107. https://doi.org/10.1186/1471-2202-13-107.

Boyd, Lara A., Winstein, Carolee J., 2006. Explicit Information Interferes with Implicit Motor Learning of Both Continuous and Discrete Movement Tasks after Stroke. Journal of Neurologic Physical Therapy. https://doi.org/10.1097/01.NPT.0000282566.48050.9b.

Buetefisch, C.M., 2015. Role of the contralesional hemisphere in post-stroke recovery of upper extremity motor function. Front. Neurol. 6 (OCT), 1–10. https://doi.org/10.3389/fneur.2015.00214.

Bundy, David T., Souders, Lauren, Baranyai, Kelly, Leonard, Laura, Schalk, Gerwin, Coker, Robert, Moran, Daniel W., Huskey, Thy, Leuthardt, Eric C., 2017. Contralesional brain-computer interface control of a powered exoskeleton for motor recovery in chronic stroke survivors. Stroke 48 (7), 1908–1915. https://doi.org/10.1161/STROKEAHA.116.016304.

Carey, James R., Kimberley, Teresa J., Lewis, Scott M., Auerbach, Edward J., Dorsey, Lisa, Rundquist, Peter, Ugurbil, Kamil, 2002. Analysis of FMRI and Finger Tracking Training in Subjects with Chronic Stroke. Brain. https://doi.org/10.1093/brain/awf091.

Cassidy, J.M., Tran, G., Quinlan, E.B., Cramer, S.C., 2018. Neuroimaging identifies patients most likely to respond to a restorative stroke therapy. Stroke 49 (2), 433–438. https://doi.org/10.1161/STROKEAHA.117.018844.

Chen, Yen Ting, Shengai Li, Craig Ditommaso, Ping Zhou, and Sheng Li. 2019. "Possible Contributions of Ipsilateral Pathways from the Contralesional Motor Cortex to the Voluntary Contraction of the Spastic Elbow Flexors in Stroke Survivors: A TMS Study." In American Journal of Physical Medicine and Rehabilitation, 98:558–65. Lippincott Williams and Wilkins. https://doi.org/10.1097/PHM.0000000000001147.

Choudhury, S., Shobhana, A., Singh, R., Sen, D., Anand, S.S., Shubham, S., Baker, M.R., Kumar, H., Baker, S.N., 2019. The Relationship Between Enhanced Reticulospinal Outflow and Upper Limb Function in Chronic Stroke Patients. Neurorehabilitation and Neural Repair 33 (5), 375–383. https://doi.org/10.1177/1545968319836233.

Dale, A.M., Fischl, B., Sereno, M.I., 1999. Cortical Surface-Based Analysis: I. Segmentation and Surface Reconstruction. NeuroImage 9 (2), 179–194. https://doi.org/10.1006/nimg.1998.0395.

Daly, J.J., McCabe, J.P., Holcomb, J., Monkiewicz, M., Gansen, J., Pundik, S., 2019. Long-Dose Intensive Therapy Is Necessary for Strong, Clinically Significant, Upper Limb Functional Gains and Retained Gains in Severe/Moderate Chronic Stroke. Neurorehabilitation and Neural Repair 33 (7), 523–537. https://doi.org/10.1177/1545968319846120.

Dick, Anthony Steven, Tremblay, Pascale, 2012. Beyond the arcuate fasciculus: consensus and controversy in the connectional anatomy of language. Brain. https://doi.org/10.1093/brain/aws222.

Dodd, K.C., Nair, V.A., Prabhakaran, V., 2017. Role of the Contralesional vs. Ipsilesional Hemisphere in Stroke Recovery. Front. Hum. Neurosci. 11 (September), 1–9. https://doi.org/10.3389/fnhum.2017.00469.

Draganski, B., May, A., 2008. Training-Induced Structural Changes in the Adult Human Brain. Behav. Brain Res. 192 (1), 137–142. https://doi.org/10.1016/j.bbr.2008.02.015.

Dromerick, A.W., Reding, M.J., 1995. Functional Outcome for Hemiparesis Hemihypesthesia and Hemianopsia, Does Lesion Location Matter. Pdf. Stroke 26 (11), 2023–2026.

Edwardson, M.A., Ding, L.i., Park, C., Lane, C.J., Nelsen, M.A., Wolf, S.L., Winstein, C.J., Dromerick, A.W., 2019. Reduced Upper Limb Recovery in Subcortical Stroke Patients with Small Prior Radiographic Stroke. Front. Neurol. 10 (MAY), 1–10. https://doi.org/10.3389/fneur.2019.00454.

Fox, R.J., Cronin, T., Lin, J., Wang, X., Sakaie, K., Ontaneda, D., Mahmoud, S.Y., Lowe, M.J., Phillips, M.D., 2011. Measuring myelin repair and axonal loss with diffusion tensor imaging. Am. J. Neuroradiol. 32 (1), 85–91. https://doi.org/10.3174/ajnr.A2238.

Hamanaka, G., Ohtomo, R., Takase, H., Lok, J., Arai, K., 2018a. Role of oligodendrocyte-neurovascular unit in white matter repair. Neurosci. Lett. 684 (June), 175–180. https://doi.org/10.1016/j.neulet.2018.07.016.

Hamanaka, G., Ohtomo, R., Takase, H., Lok, J., Arai, K., 2018b. White-Matter Repair: Interaction between Oligodendrocytes and the Neurovascular Unit. Brain Circulation 4 (3), 118. https://doi.org/10.4103/bc.bc_15_18.

Hayward, K.S., Neva, J.L., Mang, C.S., Peters, S., Wadden, K.P., Ferris, J.K., Boyd, L.A., 2017. Interhemispheric Pathways Are Important for Motor Outcome in Individuals with Chronic and Severe Upper Limb Impairment Post Stroke. Neural Plasticity 2017, 1–12. https://doi.org/10.1155/2017/4281532.

Hofer, S., Frahm, J., 2006. Topography of the Human Corpus Callosum Revisited-Comprehensive Fiber Tractography Using Diffusion Tensor Magnetic Resonance Imaging. NeuroImage 32 (3), 989–994. https://doi.org/10.1016/j.neuroimage.2006.05.044.

Hsieh, C.L., Hsueh, P., Chiang, F.M., Lin, P.H., 1998. Inter-rater reliability and validity of theaction research arm test in strokepatients. Age Ageing 27, 107–113.

Jang, S.H., Park, K.A., Ahn, S.H., Cho, Y.W., Byun, W.M., Son, S.M., Choi, J.H., Kwon, Y. H., 2009. Transcallosal Fibers from Corticospinal Tract in Patients with Cerebral Infarct. NeuroRehabilitation 24 (2), 159–164. https://doi.org/10.3233/NRE-2009-0464.

Krishnamurthi, R.V., Feigin, V.L., Forouzanfar, M.H., Mensah, G.A., Connor, M., Bennett, D.A., Moran, A.E., Sacco, R.L., Anderson, L.M., Truelsen, T., O'Donnell, M., Venketasubramanian, N., Barker-Collo, S., Lawes, C.M.M., Wang, W., Shinohara, Y., Witt, E., Ezzati, M., Naghavi, M., Murray, C., 2013. Global and Regional Burden of First-Ever Ischaemic and Haemorrhagic Stroke during 1990–2010: Findings from the Global Burden of Disease Study 2010. The Lancet Global Health 1 (5), e259–e281. https://doi.org/10.1016/S2214-109X(13)70089-5.

Króliczak, G., Piper, B.J., Frey, S.H., 2016. Specialization of the Left Supramarginal Gyrus for Hand-Independent Praxis Representation Is Not Related to Hand Dominance. Neuropsychologia 93, 501–512. https://doi.org/10.1016/j.neuropsychologia.2016.03.023.

Króliczak, Grzegorz, Piper, Brian J., Potok, Weronika, Buchwald, Mikołaj, Kleka, Paweł, Przybylski, Łukasz, Styrkowiec, Piotr P., 2020. Praxis and language organization in left-handers. Acta Neuropsychologica. https://doi.org/10.5604/01.3001.0013.9738.

Lang, C.E., Strube, M.J., Bland, M.D., Waddell, K.J., Cherry-Allen, K.M., Nudo, R.J., Dromerick, A.W., Birkenmeier, R.L., 2016. Dose Response of Task-Specific Upper Limb Training in People at Least 6 Months Poststroke: A Phase II, Single-Blind, Randomized, Controlled Trial. Ann. Neurol. 80 (3), 342–354. https://doi.org/10.1002/ana.v80.310.1002/ana.24734.

Li, S., Chen, Y.T., Francisco, G.E., Zhou, P., Rymer, W.Z., 2019. A Unifying Pathophysiological Account for Post-Stroke Spasticity and Disordered Motor Control. Front. Neurol. 10 (MAY), 1–8. https://doi.org/10.3389/fneur.2019.00468.

Li, Y., Wu, P., Liang, F., Huang, W., Yao, D., 2015. The Microstructural Status of the Corpus Callosum Is Associated with the Degree of Motor Function and Neurological Deficit in Stroke Patients. PLoS ONE 10 (4), e0122615.

Lin, L.Y., Ramsey, L., Metcalf, N.V., Rengachary, J., Shulman, G.L., Shimony, J.S., Corbetta, M., Boltze, J., 2018. Stronger Prediction of Motor Recovery and Outcome Post-Stroke by Cortico-Spinal Tract Integrity than Functional Connectivity. PLoS ONE 13 (8), e0202504. https://doi.org/10.1371/journal.pone.0202504.

Lindenberg, R., Zhu, L.L., Rüber, T., Schlaug, G., 2012. Predicting Functional Motor Potential in Chronic Stroke Patients Using Diffusion Tensor Imaging. Hum. Brain Mapp. 33 (5), 1040–1051. https://doi.org/10.1002/hbm.v33.510.1002/hbm.21266.

Lyle, R.C., 1981. A Performance Test for Assessment of Upper Limb Function in Physical Rehabilitation Treatment and Research. Int. J. Rehabil. Res. 4 (4), 483–492. https://doi.org/10.1097/00004356-198112000-00001.

McCabe, Jessica, Monkiewicz, Michelle, Holcomb, John, Pundik, Svetlana, Daly, Janis J., 2015. Comparison of robotics, functional electrical stimulation, and motor learning methods for treatment of persistent upper extremity dysfunction after stroke: a randomized controlled trial. Arch. Phys. Med. Rehabil. 96 (6), 981–990. https://doi.org/10.1016/j.apmr.2014.10.022.

McPherson, J.G., Chen, A., Ellis, M.D., Yao, J., Heckman, C.J., Dewald, J.P.A., 2018. Progressive Recruitment of Contralesional Cortico-Reticulospinal Pathways Drives

Motor Impairment Post Stroke. J. Physiol. 596 (7), 1211–1225. https://doi.org/10.1113/tjp.2018.596.issue-710.1113/JP274968.
Miyai, Ichiro, Blau, Alan D., Reding, Michael J., Volpe, Bruce T., 1997. Patients with stroke confined to basal ganglia have diminished response to rehabilitation efforts. Neurology 48 (1), 95–101. https://doi.org/10.1212/WNL.48.1.95.
O'Donnell, L.J., Westin, C.-F., 2011. An Introduction to Diffusion Tensor Image Analysis. Neurosurg. Clin. N. Am. 22 (2), 185–196. https://doi.org/10.1016/j.nec.2010.12.004.
Owen, Meriel, Carson Ingo, and Julius P.A. Dewald. 2017. "Upper Extremity Motor Impairments and Microstructural Changes in Bulbospinal Pathways in Chronic Hemiparetic Stroke." Frontiers in Neurology 8 (JUN). https://doi.org/10.3389/fneur.2017.00257.
Plow, E.B., Sankarasubramanian, V., Cunningham, D.A., Potter-Baker, K., Varnerin, N., Cohen, L.G., Sterr, A., Conforto, A.B., Machado, A.G., 2016. Models to Tailor Brain Stimulation Therapies in Stroke. Neural Plasticity 2016, 1–17. https://doi.org/10.1155/2016/4071620.
Qiu, M., Darling, W.G., Morecraft, R.J., Ni, C.C., Rajendra, J., Butler, A.J., 2011. White Matter Integrity Is a Stronger Predictor of Motor Function than BOLD Response in Patients with Stroke. Neurorehabilitation and Neural Repair 25 (3), 275–284. https://doi.org/10.1177/1545968310389183.
Rengachary, J., d'Avossa, G., Sapir, A., Shulman, G.L., Corbetta, M., 2009. Is the Posner Reaction Time Test More Accurate Than Clinical Tests in Detecting Left Neglect in Acute and Chronic Stroke? Arch. Phys. Med. Rehabil. 90 (12), 2081–2088. https://doi.org/10.1016/j.apmr.2009.07.014.
Rickards, T., Sterling, C., Taub, E., Perkins-Hu, C., Gauthier, L., Graham, M., Griffin, A., Davis, D., Mark, V.W., Uswatte, G., 2014. Diffusion Tensor Imaging Study of the Response to Constraint-Induced Movement Therapy of Children with Hemiparetic Cerebral Palsy and Adults with Chronic Stroke. Arch. Phys. Med. Rehabil. 95 (3), 506–514.e1. https://doi.org/10.1016/j.apmr.2013.08.245.
Riley, J.D., Le, V.u., Der-Yeghiaian, L., See, J., Newton, J.M., Ward, N.S., Cramer, S.C., 2011. Anatomy of Stroke Injury Predicts Gains from Therapy. Stroke 42 (2), 421–426. https://doi.org/10.1161/STROKEAHA.110.599340.
Robb, R.A., Hanson, D.P., 1991. Software System for Interactive and Quantitative Visualization of Multidimensional Biomedical Images. Australas. Phys. Eng. Sci. Med.
Schaechter, J.D., Fricker, Z.P., Perdue, K.L., Helmer, K.G., Vangel, M.G., Greve, D.N., Makris, N., 2009. Microstructural Status of Ipsilesional and Contralesional Corticospinal Tract Correlates with Motor Skill in Chronic Stroke Patients. Hum. Brain Mapp. 30 (11), 3461–3474. https://doi.org/10.1002/hbm.v30:1110.1002/hbm.20770.
Schlaug, G., Marchina, S., Norton, A., 2009. Evidence for Plasticity in White-Matter Tracts of Patients with Chronic Broca's Aphasia Undergoing Intense Intonation-Based Speech Therapy. Ann. N. Y. Acad. Sci. 1169, 385–394. https://doi.org/10.1111/j.1749-6632.2009.04587.x.
Shelton, Fátima De N.A.P., Reding, Michael J., 2001. Effect of lesion location on upper limb motor recovery after stroke. Stroke 32 (1), 107–112. https://doi.org/10.1161/01.STR.32.1.107.
Simis, M., Doruk, D., Imamura, M., Anghinah, R., Morales-Quezada, L., Fregni, F., Battistella, L.R., 2015. Neurophysiologic Predictors of Motor Function in Stroke. Restor. Neurol. Neurosci. 34 (1), 45–54. https://doi.org/10.3233/RNN-150550.
Smith, S.M., Jenkinson, M., Johansen-Berg, H., Rueckert, D., Nichols, T.E., Mackay, C.E., Watkins, K.E., Ciccarelli, O., Cader, M.Z., Matthews, P.M., Behrens, T.E.J., 2006. Tract-Based Spatial Statistics: Voxelwise Analysis of Multi-Subject Diffusion Data. NeuroImage 31 (4), 1487–1505. https://doi.org/10.1016/j.neuroimage.2006.02.024.
Song, J., Nair, V.A., Young, B.M., Walton, L.M., Nigogosyan, Z., Remsik, A., Tyler, M.E., Farrar-Edwards, D., Caldera, K.E., Sattin, J.A., Williams, J.C., Prabhakaran, V., 2015. DTI Measures Track and Predict Motor Function Outcomes in Stroke Rehabilitation Utilizing BCI Technology. Front. Hum. Neurosci. 9 https://doi.org/10.3389/fnhum.2015.00195.
Song, S.-K., Sun, S.-W., Ju, W.-K., Lin, S.-J., Cross, A.H., Neufeld, A.H., 2003. Diffusion Tensor Imaging Detects and Differentiates Axon and Myelin Degeneration in Mouse Optic Nerve after Retinal Ischemia. NeuroImage 20 (3), 1714–1722. https://doi.org/10.1016/j.neuroimage.2003.07.005.
Sterr, A., Dean, P.J.A., Szameitat, A.J., Conforto, A.B., Shen, S., 2014. Corticospinal Tract Integrity and Lesion Volume Play Different Roles in Chronic Hemiparesis and Its Improvement through Motor Practice. Neurorehabilitation and Neural Repair 28 (4), 335–343. https://doi.org/10.1177/1545968313510972.
Stewart, Jill Campbell, Pritha Dewanjee, George Tran, Erin Burke Quinlan, Lucy Dodakian, Alison McKenzie, Jill See, and Steven C. Cramer. 2017. "Role of Corpus Callosum Integrity in Arm Function Differs Based on Motor Severity after Stroke." NeuroImage: Clinical 14: 641–47. https://doi.org/10.1016/j.nicl.2017.02.023.
Stinear, C.M., Alan Barber, P., Smale, P.R., Coxon, J.P., Fleming, M.K., Byblow, W.D., 2007. Functional Potential in Chronic Stroke Patients Depends on Corticospinal Tract Integrity. Brain 130 (1), 170–180. https://doi.org/10.1093/brain/awl333.
Takeuchi, Naoyuki, and Shin-ichi Izumi. 2013. "Rehabilitation with Poststroke Motor Recovery.Pdf" 2013.
Thickbroom, Gary W., Cortes, Mar, Rykman, Avrielle, Volpe, Bruce T., Felipe Fregni, H., Krebs, Igo, Pascual-Leone, Alvaro, Edwards, Dylan J., 2015. Stroke subtype and motor impairment influence contralesional excitability. Neurology 85 (6), 517–520. https://doi.org/10.1212/WNL.0000000000001828.
Van Vliet, P., Carey, L., Nilsson, M., 2012. Targeting Stroke Treatment to the Individual. International Journal of Stroke 7 (6), 480–481. https://doi.org/10.1111/j.1747-4949.2012.00867.x.
Wadden, K. P., S. Peters, M. R. Borich, J. L. Neva, K. S. Hayward, C. S. Mang, N. J. Snow, et al. 2019. "White Matter Biomarkers Associated with Motor Change in Individuals with Stroke: A Continuous Theta Burst Stimulation Study." Neural Plasticity 2019 (di). https://doi.org/10.1155/2019/7092496.
Wan, C.Y., Zheng, X., Marchina, S., Norton, A., Schlaug, G., 2014. Intensive Therapy Induces Contralateral White Matter Changes in Chronic Stroke Patients with Broca's Aphasia. Brain Lang. 136 (July), 1–7. https://doi.org/10.1016/j.bandl.2014.03.011.
Wang, L.E., Tittgemeyer, M., Imperati, D., Diekhoff, S., Ameli, M., Fink, G.R., Grefkes, C., 2012. Degeneration of Corpus Callosum and Recovery of Motor Function after Stroke: A Multimodal Magnetic Resonance Imaging Study. Hum. Brain Mapp. 33 (12), 2941–2956. https://doi.org/10.1002/hbm.v33.1210.1002/hbm.21417.
Xu, Jing, Adrian M. Haith, and John W. Krakauer. 2015. "Motor Control of the Hand before and after Stroke." In Clinical Systems Neuroscience. https://doi.org/10.1007/978-4-431-55037-2_14.
Yeh, F.C., Panesar, S., Fernandes, D., Meola, A., Yoshino, M., Fernandez-Miranda, J.C., Vettel, J.M., Verstynen, T., 2018. Population-Averaged Atlas of the Macroscale Human Structural Connectome and Its Network Topology. NeuroImage 178, 57–68. https://doi.org/10.1016/j.neuroimage.2018.05.027.
Yeh, F.-C., Verstynen, T.D., Wang, Y., Fernández-Miranda, J.C., Tseng, W.-Y., Zhan, W., 2013. Deterministic Diffusion Fiber Tracking Improved by Quantitative Anisotropy. PLoS ONE 8 (11), e80713. https://doi.org/10.1371/journal.pone.0080713.
Young, B.M., Stamm, J.M., Song, J., Remsik, A.B., Nair, V.A., Tyler, M.E., Edwards, D.F., Caldera, K., Sattin, J.A., Williams, J.C., Prabhakaran, V., 2016. Brain-Computer Interface Training after Stroke Affects Patterns of Brain-Behavior Relationships in Corticospinal Motor Fibers. Front. Hum. Neurosci. 10 https://doi.org/10.3389/fnhum.2016.00457.
Yozbatiran, N., Der-Yeghiaian, L., Cramer, S.C., 2008. A Standardized Approach to Performing the Action Research Arm Test. Neurorehabilitation and Neural Repair 22 (1), 78–90. https://doi.org/10.1177/1545968307305353.